

Video Article

Reaction Kinetics and Combustion Dynamics of I₄O₉ and Aluminum MixturesDylan K. Smith¹, Michelle L. Pantoya¹, Jeffrey S. Parkey², Mehmet Kesmez²¹Department of Mechanical Engineering, Texas Tech University²Lynntech Inc.Correspondence to: Michelle L. Pantoya at michelle.pantoya@ttu.eduURL: <https://www.jove.com/video/54661>DOI: [doi:10.3791/54661](https://doi.org/10.3791/54661)Keywords: Engineering, Issue 117, iodine compounds, tetraiodine nonoxide, I₄O₉, reactivity, aluminum combustion, biocidal agent, iodine gas, flame speed, DSC, TGA

Date Published: 11/7/2016

Citation: Smith, D.K., Pantoya, M.L., Parkey, J.S., Kesmez, M. Reaction Kinetics and Combustion Dynamics of I₄O₉ and Aluminum Mixtures. *J. Vis. Exp.* (117), e54661, doi:10.3791/54661 (2016).

Abstract

Tetraiodine nonoxide (I₄O₉) has been synthesized using a dry approach that combines elemental oxygen and iodine without the introduction of hydrated species. The synthesis approach inhibits the topochemical effect promoting rapid hydration when exposed to the relative humidity of ambient air. This stable, amorphous, nano-particle material was analyzed using differential scanning calorimetry (DSC) and thermal gravimetric analysis (TGA) and showed an exothermic energy release at low temperature (*i.e.*, 180 °C) for the transformation of I₄O₉ into I₂O₅. This additional exothermic energy release contributes to an increase in overall reactivity of I₄O₉ when dry mixed with nano-aluminum (Al) powder, resulting in a minimum of 150% increase in flame speed compared to Al + I₂O₅. This study shows that as an oxidizer, I₄O₉ has more reactive potential than other forms of iodine(V) oxide when combined with Al, especially if I₄O₉ can be passivated to inhibit absorption of water from its surrounding environment.

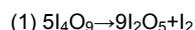
Video Link

The video component of this article can be found at <https://www.jove.com/video/54661/>

Introduction

There are many iodine oxide compounds (*e.g.*, HIO₃, HI₃O₈, I₂O₅, I₄O₉) but the one most commonly studied for reaction with aluminum (Al) is diiodide pentoxide, I₂O₅¹⁻¹⁶. There are reasons for favoring I₂O₅ for combustion with Al: (1) I₂O₅ has an oxidation state of five which makes it a strong oxidizer for combustion applications; (2) I₂O₅ is semi-stable, depending on atmospheric conditions, and easily handled in powder form; and (3) I₂O₅ is relatively easy to produce and readily available.

Other forms of iodine oxide that have been studied are HIO₃, HI₃O₈, and I₄O₉. When heated to low temperatures (*i.e.*, 180 °C), I₄O₉ thermally decomposes into I₂O₅⁶ as shown in Equation (1) and the decomposition reaction is exothermic.

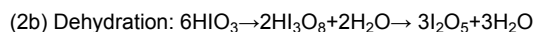
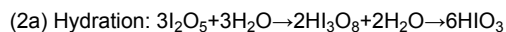


If I₄O₉ could be used in place of I₂O₅, the total energy liberated from reaction could increase due to the exothermic decomposition of I₄O₉ at temperatures below the Al ignition and reaction temperatures (*i.e.*, < 660 °C) and below the dissociation temperature of I₂O₅ (*i.e.*, about 350 °C). Also, I₄O₉ generates 8 wt.% more I₂ gas when compared to I₂O₅ that could be used to neutralize biological agents. However, I₄O₉ has a higher molecular weight when compared to I₂O₅ and it is unknown if more energy is released per mass or per volume when using I₄O₉ compared to I₂O₅. Using I₄O₉ could provide a way to transport large quantities of solid iodine and upon ignition, release gaseous iodine. But, I₄O₉ powder is usually unstable. In fact, Wikjord *et al.*⁶ showed that over very short times I₄O₉ decomposed into I₂O₅ even with limited exposure to the atmosphere. This instability limits the usefulness of I₄O₉ as an oxidizer in combustion applications.

Iodic acids, such as HIO₃ and HI₃O₈, form when I₂O₅ is exposed to water either from the relative humidity (RH) of the atmosphere or from immersion in a fluid^{1,3}. For combustion applications, I₂O₅ is usually preferred over the hydrated iodic acids because evaporation of water upon combustion absorbs energy and reduces the overall heat produced. Despite the endothermic nature of this phase change, Smith *et al.*³ showed rapid evaporation of water during combustion of Al with I₂O₅ comprised partially of iodic acids produced significant gas generation that increased convective energy transport and produced higher flame speeds than Al + I₂O₅ alone. Specifically, mixtures with higher concentrations of iodic acids had up to 300% higher flame speeds than mixtures with lower concentrations of iodic acids.³

The rate of absorption from atmospheric water is dependent on RH. There is a RH threshold where absorption begins and dependent on the hydration state². Little *et al.* showed a RH threshold of 70% for HIO₃ and a RH threshold of 40% for HI₃O₈². From this, it is assumed that the RH threshold increases with increasing hydration states. Because of its deliquescent properties, most studies that use I₂O₅ as an oxidizer are actually using I₂O₅ with significant concentrations of iodic acid^{2,5,7,17}. However, the initial concentrations of the samples can be controlled by

heating the samples above 210 °C until all of the hydrated species have dehydrated. This follows the hydration and dehydration mechanism of I_2O_5 shown in Selte *et al.*¹ in Equation (2).



The first step in dehydration happens at 110 °C when HIO_3 dehydrates into HI_3O_8 . The second step of dehydration happens at 210 °C when HI_3O_8 dehydrates into I_2O_5 . Because the initial concentration of commercially available I_2O_5 is composed mostly of iodic acids, the absorption characteristics of pure I_2O_5 have not been studied thoroughly. It is assumed that the RH threshold and absorption rates are dependent on physical properties (*i.e.*, particle size, crystal structure) along with initial hydration state and that an iodine oxide that is amorphous may have a lower RH threshold and increased hydration rates. Isolating iodine oxides from atmospheric water is needed to control the initial state of iodine oxide compounds. One method of isolating I_2O_5 from the atmosphere is blocking water absorption with coatings. For example, Little *et al.* was able to reduce the absorption rate and total amount of hydrated iodine oxides by sputter coating samples with Au/Pd². Feng *et al.*⁸ passivated the surface of I_2O_5 particles with an Fe_2O_3 coating which prevented water absorption over long durations of exposure to ambient atmosphere. A similar approach could be applied to help stabilize I_4O_9 .

Another way to improve the stability of I_4O_9 may be new approaches for its synthesis. If the material could be synthesized in a way that prevents introduction of hydrated species, then the topochemical effect that catalyzes water absorption could be inhibited thereby stabilizing the oxidizer. The I_4O_9 examined here was synthesized using a 'dry' process that does not introduce hydrated species and enables analysis of a more stable form of I_4O_9 powder. Our objective is to analyze the fundamental kinetics associated with I_4O_9 decomposition and reaction with Al as well as the basic energy propagation behavior of the Al + I_4O_9 reaction. Reaction kinetics are analyzed using thermal equilibrium diagnostics including differential scanning calorimetry and thermal gravimetric analysis (DSC-TGA). Energy propagation is analyzed using high speed imaging of reaction propagation through a powder mixture upon ignition in a transparent tube. Development of synthesis methods to produce I_4O_9 and methods to stabilize I_4O_9 have been slow in comparison to other forms of iodine oxide. A goal of this study is to show that the energy and gas liberated from reactions involving I_4O_9 are greater than reactions involving other iodine oxides. In this way, future research on synthesis and characterization of I_4O_9 may be beneficial for many applications.

Protocol

NOTE: Six different oxidizers were investigated for the purpose of characterizing the kinetics of I_4O_9 in comparison to other iodine oxides. Each oxidizer is described below. The fuel used for all mixtures was constant: Al powder with 80 nm average spherical particle diameter. Mixture preparation is described following discussion of each oxidizer.

1. Preparation of Iodine(V) Oxides

NOTE: Nano-aluminum/oxidizer mixtures are highly volatile and can exhibit explosive behavior. These mixtures are susceptible to unintended ignition by electrostatic discharge, friction, impact, and other forms of accidental ignition. All equipment should be grounded to decrease the likelihood of accidental spark ignition. Quantities should be minimized and protective equipment should be used when handling these materials. More information on safety and handling procedures can be found in Maienschein *et al.*¹⁸

1. Preparation commercial I_2O_5

1. Crush 10 g of I_2O_5 crystals with a mortar and pestle until a consistent powder is created.
2. After the crystals are in a powder form, evenly spread the 10 g of powder in a ceramic crucible suitable for heating up to 250 °C.
3. Place entire crucible in an oven and heat to 250 °C at 10°C/min and hold at 250 °C for 5 min.

2. Preparation of amorphous I_2O_5

1. Place 3 g of the crushed and dehydrated commercial I_2O_5 in a glass beaker with a magnetic stirrer and add 3 g of distilled water. To ensure the sample is completely dissolved, add a 1:1 ratio of water to commercial I_2O_5 and mix for 20 min. Dissolution of I_2O_5 in water forms an aqueous phase of IO_3 .¹⁷
2. Pour the IO_3 solution into a beaker that is suitable for heating. To ensure enough amorphous I_2O_5 is produced, use three times the mass of IO_3 solution than the mass needed of amorphous I_2O_5 . For example, if one gram of amorphous I_2O_5 is needed, use 3 g of IO_3 solution.
3. Place the beaker with the IO_3 solution into an oven and heat at 20 °C/min to 250 °C and hold for 10 min.
4. Store the sample in a sealed container to limit exposure to atmospheric water from the environment.

3. Preparation crystalline HIO_3

1. Repeat step 1.2.1 and place IO_3 solution on a magnetic stirrer in a low humidity environment (below 50% RH) until all of the excess water has evaporated. Upon evaporation, the aqueous phase of IO_3 will precipitate out as HIO_3 .¹⁷
2. Store the sample in a sealed container to limit exposure to atmospheric water from the environment.
3. To ensure all excess water is evaporated, place a sample into a differential scanning calorimeter (DSC) and heat to 250 °C at 10 °C/min.

NOTE: The weight loss at 110 °C will equal 5% and there will be no mass loss at 210 °C if the sample is pure HIO_3 . Any additional mass loss is excess water, which means the sample needs more time to evaporate. Weight loss at 210 °C means the I_2O_5 has not completely dissolved and more water with agitation is needed to dissolve the sample.

2. Mixture Preparation

NOTE: The mixtures are prepared in two different ways: one using a carrier fluid to aid in intermixing and another without a carrier fluid but instead dry mixed. For processing using a carrier fluid, mixtures were prepared for only three oxidizers: I_4O_9 , nano I_2O_5 and commercial I_2O_5 .

1. Preparation of mixtures in a carrier fluid

- To prepare the samples mixed in a carrier fluid, mix 80 nm Al powder with each oxidizer for a total of two grams of Al and oxidizer mixture to an equivalence ratio of 1.0 in a beaker.
- Add 60 ml of isopropanol into the beaker and sonicate the solution with a sonic wand set at an output power of 4 watts programmed for 10 sec on and 10 sec off for a total of 2 min.
- Pour solution into a glass dish and allow the solution to evaporate in a fume hood at room temperature with a relative humidity of 20% for 24 hr, which will leave powder samples.
NOTE: Before proceeding with step 2.1.4, assure razor blade is connected to an electrical ground with a conductive wire to avoid accidental ignition.
- Reclaim the powder with a grounded razor blade and sieve the sample to break up agglomerates directly into a container that can be sealed to limit sample exposure to atmospheric water.

2. Preparation of dry mixed samples

- Sieve and mix two grams of Al and oxidizer mixture with a spatula into a sample container to a fuel to oxygen equivalence ratio of 1.0. Seal the sample container to limit sample exposure to atmospheric water.
- Hold samples on a vibration table for 3 minute to aid intermixing. Refer to samples prepared in this way as dry mixed.

3. Thermal Equilibrium Analysis

1. Preparation of samples for thermal equilibrium analysis

NOTE: These samples react easily with atmospheric water. Relative humidity should be reduced below 30% and exposure to the atmosphere should be limited (*i.e.*, store sample in sealed containers and use lids on DSC-TGA crucibles).

- Heat alumina crucibles (supplied with the DSC-TGA diagnostic) to 1,500 °C and hold for 30 min to remove any residue on the crucibles in the DSC-TGA.
- Weigh crucibles before the samples are placed in the crucible. This measurement is needed by the DSC-TGA.
- After the crucible is weighed, add 10 mg of each sample into a crucible.
- Place the sample crucible on the thermocouple in the DSC-TGA with an empty crucible in the reference holder on the DSC thermocouple.
- Heat the samples at 10 °C/min to 600 °C in an argon atmosphere.

4. Energy Propagation

1. Preparation of flame tubes

- Use quartz tubes with an inside diameter of 3 mm and length of 7 cm to contain the powder mixture.
- Put tape on one end so powder cannot escape from the tube.
- Place each 7 cm tube with one end taped on a scale and zero the scale. This will allow the measurement of just the mass of powder.
- Using a spatula with a small end, insert the powder samples into the tube. For each of the mixtures, make three tubes filled with each mixture for repeatability testing.
- Using a rod that has a diameter smaller than 3 mm, compact the powder inside the tube for the samples with low bulk densities (*i.e.*, Al + I_4O_9 and Al + amorphous I_2O_5) until the volume of the sample does not change. This procedure is necessary to maintain consistent bulk densities between multiple experiments. This may require 200 mg of powder mixture.
- For all other mixtures, which have higher densities, do not compact the powder using external force. Keep the bulk density constant between samples with similar bulk densities. The amount of powder in the tubes will vary depending on bulk density of the powder. This may require up to 500 mg of powder mixture.
- Measure the mass of powder mixture in each tube using the balance that was tared for each tube, add mass until the density of the powder is within 5% of the other samples in each group. Make sure each tube is completely filled.

2. Preparation of hot wire ignite

- To prepare the hot wire, use a nickel-chromium (*i.e.*, nichrome) wire cut into sections 10 cm long.
- Make a "v" shape in the middle of the wire and place the wire so the "v" shape is inside the tube.
- Tape this end of the tube so the wire is stationary and no powder can escape the tube.

3. Preparation of high speed camera

- Place the high speed camera outside the combustion chamber perpendicular to the direction of flame propagation and focus the camera on the tube through a viewing port in the combustion chamber.
NOTE: The primary function of the combustion chamber is to protect personnel and equipment from the reacting material and should be ventilated through a fume hood.
- Adjust placement and lens of the camera so the lowest resolution (*i.e.*, highest frame rate) can be used.
- To allow distance calibration, place a ruler with mm and cm increments in the field of view and take a snapshot with the high speed camera prior to recording flame speeds.
- As the flame front is significantly brighter than ambient light and the camera will over-saturate when exposed to the light generated by the reaction, lower the exposure time in the camera settings or add neutral density filters to the lens of the camera to reduce the

- amount of light received by the camera sensors. Lower the amount of light received by the camera until the propagation front of the reaction can be seen clearly. Here, set up neutral density filters allowing only 5% of the light to pass, and an exposure time of 1 μ sec.
- Attach a voltage generator to the ends of the wire. The combustion chamber should have insulated leads through the chamber which will allow the chamber to be sealed and allow remote heating of the wire.
 - After the chamber is sealed, set the voltage generator to 10 volts and simultaneously begin the camera recording. When the voltage is applied, the reaction should start almost immediately.
 - Export the video into a software program that will track the position of the flame front as a function of time in each individual frame.
 - Export the distance and time step information into a spread sheet and plot a linear trend line with R^2 values. For slower reactions, time is needed for the reaction to reach a steady state. The curve before the steady state will be an exponentially increasing curve. Remove the data that are not in steady state until the R^2 value is greater than 0.95. The slope of the line is the flame speed.

Representative Results

Figure 1a shows the endothermic and exothermic behavior of the initial states for all six oxidizers examined from DSC analysis and **Figure 1b** shows the corresponding mass loss from TGA analysis. It is noted that all oxidizers when heated beyond the dissociation temperature of I_2O_5 (350 °C) lose 100% mass but the I_4O_9 sample releases I_2 gas instead of water liberated by dehydration of hydrated species at temperatures below the dissociation temperature of I_2O_5 . The abundance of I_2 gas released from the I_4O_9 samples is specified in **Figure 1b** at over 7 wt.%. **Figure 1a** shows that the only iodine compounds that produce exothermic behavior is I_4O_9 and I_2O_5 formed by decomposition of I_4O_9 , and the exotherm corresponds to an onset temperature of about 180 °C for decomposition into I_2O_5 . **Figure 1b** also shows that the iodine compound with the greatest overall iodine gas generation is I_4O_9 .

There are no endotherms for commercial and amorphous I_2O_5 samples between 110 °C and 210 °C. This shows that these samples are purely I_2O_5 with no iodic acids. The nano I_2O_5 and I_4O_9 have exotherms with onset temperature at 150 °C. This shows those samples contain I_4O_9 . The nano I_2O_5 is thermally treated I_4O_9 . The small exotherm at 150 °C shows that there is some residual I_4O_9 in the nano I_2O_5 sample. Using the TGA data from **Figure 1b**, the residual I_4O_9 in the sample is less than 15 wt.%. The HIO_3 dehydrate has a single endotherm starting at 130 °C and indicates this sample is crystalline HIO_3 . The commercial HIO_3 sample has two distinct endotherms starting at 160 °C and 210 °C. An endotherm with an onset temperature of 160 °C is outside of the range of HIO_3 dehydration in the CRC handbook¹⁶. However, TGA results show a mass loss of 2.47 wt.% over this range indicating it is the dehydration of a hydrated species.

Figure 2a shows the heat flow behavior from DSC analysis of four Al and iodine oxide mixtures. The Al + I_4O_9 dry mixture has an exotherm at 180 °C indicating the oxidizer is still I_4O_9 with an increased onset temperature. The Al + I_4O_9 and Al + nano I_2O_5 samples are almost identical. Both of these mixtures were processed using isopropanol as the carrier fluid to aid intermixing and identical thermal behavior seen in **Figure 2a** indicating that mixing powders in isopropanol transformed I_4O_9 into I_2O_5 .

Figure 2b shows I_4O_9 , I_4O_9 exposed to 20% RH for 4 hours, and nano I_2O_5 exposed to 20% RH for 4 hours. After 4 hours exposure to 20% RH, I_4O_9 is identical to nano I_2O_5 and there are endotherms at 110 °C and 210 °C showing the samples are partially composed of HIO_3 and HI_3O_8 . This may be explained by the I_4O_9 "dry" synthesis method which is then heated and transformed into I_2O_5 . The crystal structure of I_4O_9 is not known, but because hydration is observed (**Figure 2b** bottom two curves with endotherms shaded), the low density of the powder (*i.e.*, fluffy, highly porous nature), and the lack of a reported crystalline structure, an amorphous structure is assumed. Nano I_2O_5 is formed by thermal decomposition of amorphous I_4O_9 , according to Eq. (1) such that I_2 is released from amorphous I_4O_9 leaving amorphous I_2O_5 . Crystal structure formation of iodine(V) oxides is catalyzed by water. Since the synthesis method is dry, there is no water to catalyze crystal formation. The first step required for absorption of water is to raise the relative humidity to disrupt the bonds between molecules. Without this crystal structure (that wants to release the weakly bonded water) the dynamic equilibrium is shifted so I_2O_5 will absorb any available water. As soon as water is absorbed by I_2O_5 , formation of HIO_3 molecules begin. HIO_3 has a hydrogen that attracts oxygen in amorphous I_2O_5 and creates an HI_3O_8 crystal structure. Water is still the catalyst in crystal structure formation. The synthesis method of I_2O_5 and I_4O_9 which form an amorphous structure instead of a crystalline structure is the reason water absorption is seen at lower RH (*i.e.*, 20%) than what was required to start absorption in previous studies (*i.e.*, 70-80% RH)^{5,17}. In summary, the iodine compounds' amorphous structure may promote absorption of hydrated species and formation of iodic acids.

In **Figure 2a** the main exotherms around 500 °C are all similar. In the Al + I_4O_9 dry mix, the exotherm at about 180 °C indicates phase transition from I_4O_9 to I_2O_5 . Also, all mixtures have a pre-ignition reaction (PIR) between 300 - 400 °C, but Al + I_4O_9 and Al + nano I_2O_5 have a PIR with lower onset temperature and greater magnitude but also show unique endotherms followed by exotherms at 210 °C. These samples were processed in isopropanol and the behavior at 210 °C indicates these samples are partially HI_3O_8 . The exotherm may be reaction between HI_3O_8 and I_4O_9 because HI_3O_8 is dissociating at nearly the same temperature as I_4O_9 decomposition. These reactions may help promote greater exothermicity in the PIR and catalyze earlier onset of the PIR. Osborne and Pantoya²⁰ first showed an exothermic reaction preceding the main exothermic reaction in Al combustion and coined this a PIR. Their analysis indicated the PIR reaction was between the alumina shell surrounding an aluminum core particle with fluorine from decomposing fluoropolymer^{19,20}. Farley *et al.*⁴ then extended observations of the PIR to aluminum-alumina core-shell particles reacting with iodine based oxidizers. The Al + commercial I_2O_5 sample has an endotherm at 210 °C indicating HI_3O_8 presence and a mild PIR exotherm with delayed onset temperature. Mulamba *et al.*²¹ also showed that the PIR onset temperature is concentration dependent.

Table 1 shows measured flame speed results for Al mixed with the indicated oxidizer as a dry mixture and also mixed using isopropanol as the processing carrier fluid. Only the first three samples were tested after being mixed in isopropanol and the Al + commercial HIO_3 dry mix either did not ignite or did not sustain reaction long enough to obtain measureable results. The percent uncertainty is determined based on repeatability of up to three separate experiments for each mixture. Bulk density is determined as a function of mixture powder mass and volume of the tube.

When interpreting reactivity with flame speed measurements, there are many factors that influence results such as homogeneity of the mixture, particle size, and bulk density. Mixture homogeneity can be optimized using a carrier fluid to aid intermixing of the reactants. The I_4O_9 examined in this study is more stable than previously studied I_4O_9 samples and did not appear to decompose into I_2O_5 or form hydrated species seen in Wikjord *et al.*⁶ (as seen in **Figure 1a** with only an exotherm corresponding to I_4O_9 decomposition). However, the only way to observe the combustion performance of Al + I_4O_9 is by dry mixing with as little exposure to the atmosphere as possible in order to maintain the integrity of I_4O_9 . Additionally, the flame speed measurements of Al with the oxidizers in different states allowed us to narrow the effects that cause variance in flame speed results and reveal differences attributed specifically to particular iodine compounds. These comparisons will be discussed below. Overall **Table 1** shows that I_4O_9 significantly improves reactivity when compared with other iodine compounds.

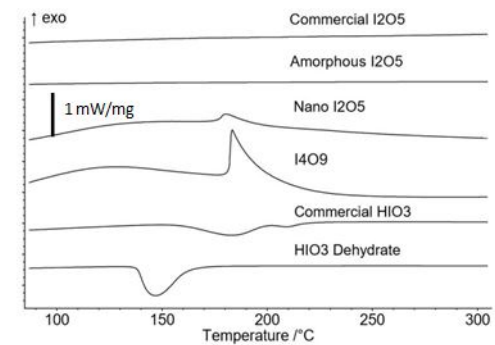
Mixing in a carrier fluid provides improved distribution of fuel and oxidizer particles that increases mixture homogeneity and reactivity. This is seen in the difference in flame speeds in **Table 1** for the dry and isopropanol mixed Al + nano I_2O_5 and Al + commercial I_2O_5 samples where the flame speeds increased by 1.07 and 3.34 times, respectively. Mixture homogeneity implicit from the measured flame speed is only slightly improved for the Al + nano I_2O_5 mixture, whereas the Al + micron scale commercial I_2O_5 exhibits a three times increase in flame speed when the carrier fluid aids intermixing. Clearly particle size and carrier fluid contribute to measured flame speed. The homogeneity effects can also be seen by the uncertainty between flame speeds. The samples that are mixed in isopropanol and the samples with smaller particles have less uncertainty in measured flame speeds. This small uncertainty is also seen in all of the amorphous samples, which suggests that an amorphous structure facilitates improved homogeneity in dry mixing. It is further noted that each sample was sieved before dry mixing to break up agglomerates and help eliminate uncertainty caused by poor homogeneity.

The HIO_3 molecules have a hydrogen end cap, which is electropositive, and an oxygen end cap, which is electronegative and causes an attraction between the ends of individual HIO_3 molecules²². Because of this attraction, during sieving the HIO_3 particles instantly agglomerated before the Al can be mixed. This caused extremely poor homogeneity and is the reason Al + commercial HIO_3 samples could not sustain the reaction. The Al + HIO_3 dehydrate sample had water available to catalyze crystal structure formation (**Figure 1a**), which reduced, but did not eliminate this effect.

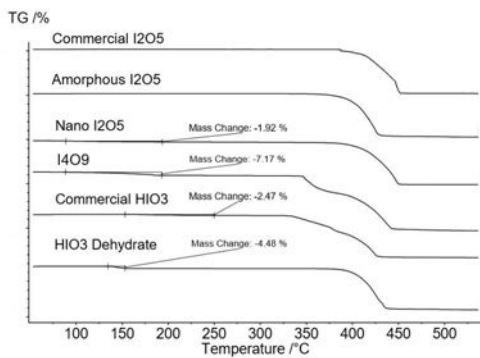
Energy propagation is dependent on the bulk density of the reactant mixture. The density will change based on the concentration of the reactants, so the bulk density of the mixture is usually reported as the percentage of the theoretical maximum density (TMD). The %TMD is calculated using a weighted average of the concentration and the densities of the reactants and accounts for the density of the actual sample according to its mass and volume occupied. In this way, bulk density in terms of %TMD represents the amount of solid space occupied by the volume (*i.e.*, 60% TMD is equivalent to 40% air voids and 60% solids). Low %TMD usually result in higher flame speeds than high %TMD powders. The higher concentration of air voids with lower %TMD provide convective pathways to enhance flame speeds. For this reason, the flame speeds reported in **Table 1** are not comparable as a function of mixture, because each was prepared at a discretely different bulk density.

Two conclusions can be drawn from **Table 1**: (1) I_4O_9 cannot be processed in isopropanol because it changes into I_2O_5 and thus alters its reactivity; and (2) I_4O_9 is more reactive than I_2O_5 because at higher and lower bulk densities (*i.e.*, 11% TMD compared with 8 or 17% TMD), I_4O_9 demonstrates increased reactivity. This finding suggests that I_4O_9 would be advantageous for reactive applications if it could be passivated to improve stability.

Through reactivity and thermal analysis, results show I_4O_9 can be more reactive than other forms of iodine(V) oxides when combined with aluminum (Al) powder. The I_4O_9 sample used here was synthesized using a 'dry' method that combines elemental oxygen and iodine such that hydrated species are not introduced at any point during synthesis. For this reason, the I_4O_9 sample is initially devoid of iodic acids and produces a large exotherm at a low temperature (*i.e.*, 180 °C) corresponding to its decomposition into I_2O_5 . The nano-scale I_2O_5 particles that are created by thermal decomposition of I_4O_9 are likely amorphous and produce flame speeds over 1,000 m/sec when combined with Al powder (**Table 1**). The Al + I_4O_9 reaction produces flame speeds over 1,500 m/sec. This is the first study to explore the potential of I_4O_9 as an alternative to I_2O_5 for energy generation technologies, especially motivated by high iodine gas generation.



a)



b)

Figure 1. DSC Analysis of Heat Flow / TGA Analysis of Mass Loss. a) Heat flow behavior from DSC analysis of six oxidizers and shows different states of iodine(V) oxides used in the range of iodic acid dehydration. b) Mass loss from corresponding TG analysis.

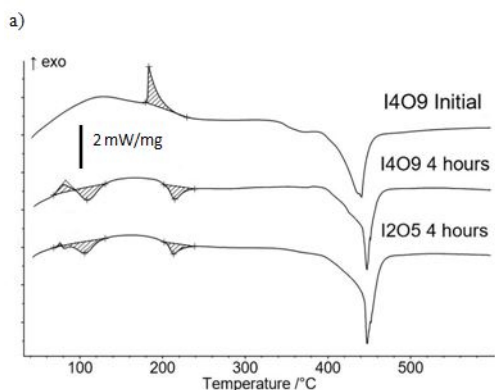
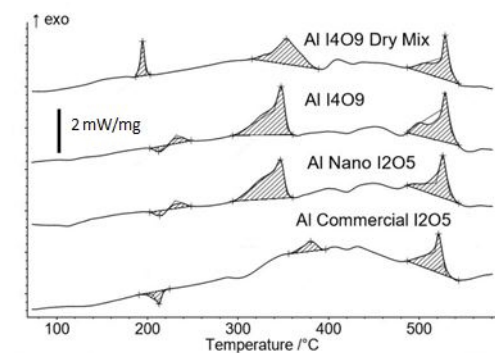


Figure 2. DSC Analysis of Heat flow. a) Heat flow behavior from DSC analysis for Al + I₄O₉ dry mix and Al + I₄O₉, Al + nano I₂O₅ and Al + commercial I₂O₅ mixed in isopropanol. Temperature range includes iodic acid dehydration and main reaction temperature range. b) I₄O₉ initially and I₄O₉ exposed to 20% RH for 4 hours. Also, the I₂O₅ was exposed to 20% RH for 4 hours.

Oxidizer	Isopropanol Mixed Flame Speed (m/sec)	% Uncertainty	Dry Mix Flame Speed	% Uncertainty	Bulk Density Dry Mix (g/cm ³)	Dry Mix %TMD
I ₄ O ₉	1,261*	0.4	1,551	3	0.48	11.7
Nano I ₂ O ₅	1,146	4.5	1,070	3.7	0.33	8
Commercial I ₂ O ₅	719	5.5	215	46.5	0.93	22.6
Amorphous I ₂ O ₅	NM	NM	1,085	0.3	0.73	17.8
HIO ₃ Dehydrate	NM	NM	393	12	0.8	19.3
Commercial HIO ₃	NM	NM	NM	NM	1.11	27.1

Table 1. Flame Speed Results. Flame speed results for Al + oxidizer indicated in first column. NM indicates not measurable. * Indicates I₄O₉ was decomposed into I₂O₅ during mixing.

Discussion

The I₄O₉ powder studied here was synthesized using a "dry" approach to form I₄O₉ by combining elemental iodine and oxygen. This sample is referred to as I₄O₉. Nano-particle I₂O₅ was also synthesized for this study. Specifically, a portion of I₄O₉ was heated past the dissociation temperature of I₄O₉ (*i.e.*, 180 °C) but under the dissociation temperature of I₂O₅ (400 °C). This process results in particles with a diameter between 200-400 nm. This sample is referred to as nano I₂O₅. Particle size measurements were obtained by TEM which requires the sample to be in a vacuum. However, I₄O₉ dissociates into I₂O₅ in a vacuum, so dimensions of I₄O₉ were not obtained directly. Because the nano I₂O₅ particle diameters are between 200-400 nm and synthesized by heating the I₄O₉ sample, it is assumed that I₄O₉ has similar diameters.

A more common approach to synthesizing I₂O₅ is by thermal dehydration of iodic acid to form I₂O₅^{1,2,8} and material made using this process is commercially available. The commercial I₂O₅ is received as coarse crystals and can have different concentrations of iodic acids depending on storage and handling conditions. To ensure samples are pure I₂O₅, the samples are dehydrated prior to use as explained in step 2.1.1.3. The diameter of the particles in this sample are between 1-5µm. This sample is referred to as commercial I₂O₅.

The amorphous I₂O₅ sample is made from this saturated IO₃ solution. When I₂O₅ is mixed with water, a solution of IO₃ is created. This is done in step 2.1.2 and these steps will leave a saturated IO₃ solution. Water catalyzes the formation of crystals in iodic acids. To form amorphous I₂O₅

the temperature must be above the dehydration temperature of HI_3O_8 and heated at a rate that will not allow a crystal structure to form, this is done in step 1.2. The concentration of IO_3 in solution will determine the amount of amorphous I_2O_5 created during dehydration. These samples should turn red after dehydration indicating the sample is an amorphous form of I_2O_5 . This sample is referred to as amorphous I_2O_5 . Also, XRD analysis (not included) was performed and confirmed the amorphous structure of the I_4O_9 and amorphous I_2O_5 samples.

When in solution, HIO_3 will release excess water and create a crystal structure. The time needed to evaporate the excess water is dependent on the size of the beaker, RH, and concentration of the IO_3 solution. In our lab at 20% RH mixing in the manner discussed above, 3-5 days were required to evaporate excess water from the samples. The solution will turn into a solid clear crystal. This process is shown in step 2.1.3 and the sample referred to as HIO_3 dehydrate. Iodic acid will be referred to as commercial HIO_3 .

When exposed to solution or atmospheric water, iodine(V) oxide undergoes chemical reactions that change the composition of the final product. To mitigate this transformation, all six oxides are also mixed with Al without solution.

Thermal analysis using DSC-TGA was calibrated in an argon atmosphere using samples with known onset temperatures and mass losses. A flame tube apparatus known as a Bockmon Tube²³ is used to measure flame speeds. Flame speed experiments are sensitive to the bulk density of the mixture. Pantoya *et al.* showed that for nano-Al based thermites, increasing bulk density can suppress the Al reaction mechanism and reduced the role of convective energy transport thereby retarding flame speed²⁴. For this reason, experiments performed for different mixtures are usually designed to keep a constant bulk density. However, the physical and chemical properties of the oxidizers examined here vary dramatically such that it was not possible to obtain consistent bulk density with all six dry mixtures. Because of this, multiple iodine oxides with different physical and chemical properties are tested to provide a basis of comparison which includes differences in %TMD, crystal structure, and hydration states. After the powder has been placed inside the tubes and measured, hot wire is used to remotely ignite the mixture.

After the flame tubes are prepared with powder mixture, flame speeds are measured in a combustion chamber using a high-speed camera. The frame rate of the camera can be increased by lowering the resolution. Reducing the resolution to increase frame rate will produce less error than higher resolution at a slower frame rate. This is why, in step 4.2.2, the lowest resolution that can still image the entire flame tube is used, this will increase the maximum frames per second the camera can record without losing information. For our chamber, a resolution of 256 x 86 was used which allowed the camera to record at 300,000 fps.

Quantifying flame speeds in highly reactive mixtures is inherently difficult because of the large number of variables that can influence reactivity (*i.e.*, mixture homogeneity, particle size, density, propagation direction, propagation velocity, *etc.*). By using a quartz tube with an inside diameter less than 4 mm in combination with a high speed camera with neutral density filters, the direction of propagation is controlled (*i.e.*, 1-D) and the amount of light that is received by the camera can be reduced to a minimum threshold such that the leading edge of light emitted by the reaction can be seen and measured clearly. This measurement assumes that the progression of this low light level is at the same rate as the reaction front. For this reason, photodiodes may not be as accurate for tracking the reaction propagation because the high light intensity of emission may cause light to travel and saturate the sensors faster than the reaction. Also, the first 1-2 cm of tube length is considered an entrance region, or region of unsteady or accelerating propagation. Linear measurements of distance as a function of time must be taken beyond this entry region to determine steady state flame speed.

The DSC/TGA is a thermal equilibrium analysis that shows detailed reaction kinetics that cannot be observed in highly reactive materials (*i.e.*, cannot be observed under non thermal equilibrium conditions). The combination of DSC/TGA analysis and flame speeds give specific information on differences in the reaction kinetics that may have implications for differences in the flame speed results. Because of this, the combination of these two measurement methods is a powerful tool for understanding and controlling highly reactive materials.

Disclosures

All authors have no competing financial interests or other conflicts of interest.

Acknowledgements

The authors Smith and Pantoya are grateful for partial support from DTRA under award HDTRA1-15-1-0029; and, ARO (and Dr. Ralph Anthenien) under award W911NF-14-1-0250 and equipment grant W911NF-14-10417. The authors J. Parkey and M. Kesmez are grateful for support from DTRA under award HDTRA1-15-P-0037. Thank you to Dr. Douglas Allen Dalton for helpful discussion.

References

1. Selte, K., Kjekshus, A. Iodine Oxides Part II on the system H_2O I_2O_5 . *Acta. Chem. Scand.* **22**, 3309-3320 (1968).
2. Little, B. K., Emery, S. B., Nittinger, J. C., Fantasia, R. C., Lindsay, C. M. Physiochemical Characterization of Iodine (V) Oxide, Part 1: Hydration Rates. (V), *Propell. Explos. Pyrot.* **40**, 595-603 (2015).
3. Smith, D. K., McCollum, J., Pantoya, M. L. Effect of Environment of Iodine Oxidation State on Reactivity with Aluminum. *Phys. Chem. Chem. Phys.* **18**, 11243-11250 (2016).
4. Farley, C., Pantoya, M. Reaction kinetics of nanometric aluminum and iodine pentoxide. *J. Therm. Anal. Calorim.* **02** (2), 609-613 (2010).
5. Little, B. K., Emery, S. B., Lindsay, M. C. Physiochemical Characterization of Iodine (V) Oxide Part II Morphology and Crystal Structure of Particulate Films. *Crystals.* **05** (4), 534-550 (2015).
6. Wikjord, A., Taylor, P., Torgerson, D., Hachkowski, L. Thermal behaviour of Corona-Precipitated Iodine Oxides. *Thermochim. Acta.* **36**, 367-375 (1980).
7. Little, B. K., *et al.* Chemical dynamics of nano-aluminum/iodine (V) oxide. *J. Phys. Conf. Ser.* **500** (5), 052025 (2014).
8. Feng, J., Jian, G., Liu, Q., Zachariah, M. R. Passivated iodine pentoxide oxidizer for potential biocidal nanoenergetic applications. *ACS Appl. Mater. Inter.* **5** (18), 8875-80 (2013).

9. Wang, H., DeLisio, J. B., Jian, G., Zhou, W., Zachariah, M. R. Electro spray formation and combustion characteristics of iodine-containing Al/CuO nanothermite microparticles. *Combust. Flame*. **162** (7), 2823-2829 (2015).
10. Sunder, S., Wren, J. C., Vikis, A. C. Raman Spectra of I_4O_9 Formed by the Reaction of Iodine with Ozone. *J. Raman Spectrosc.* **16** (6), 424-426 (1985).
11. Selte, K., Kjekshus, A. Iodine Oxides Part III. The Crystal Structure of I_2O_5 . *Acta. Chem. Scand.* **6** (24), 1913-1924 (1970).
12. Sherwood, P. M. A. X-Ray Photoelectron Spectroscopic Studies of Some Iodine Compounds. *J. Chem. Soc.* **72**, 1805-1820 (1976).
13. Russell, R., Bless, S., Pantoya, M. Impact-Driven Thermite Reactions with Iodine Pentoxide and Silver Oxide. *J. Energ. Mater.* **29** (2), 175-192 (2011).
14. Skulski, L. Organic iodine(I, III, and V) chemistry: 10 Years of development at the Medical University of Warsaw, Poland. *Molecules.* **5** (12), 1331-1371 (2000).
15. Nicolaou, K. C., Montagnon, T., Baran, P. S. HIO_3 and I_2O_5 : Mild and Selective Alternative Reagents to IBX for the Dehydrogenation of Aldehydes and Ketones. *Angew. Chem. Int. Edit.* **293** (8), 1386-1389 (2002).
16. Lide, D. R. CRC Handbook of Chemistry and Physics. CRC Press. Boca Raton, FL, 3485 (2005).
17. Kumar, R., Saunders, R. W., Mahajan, a. S., Plane, J. M. C., Murray, B. J. Physical properties of iodate solutions and the deliquescence of crystalline I_2O_5 and HIO_3 . *Atmos. Chem. Phys.* **10** (24), 12251-12260 (2010).
18. Maienschein, J., Pantoya, M. L. Safety in Energetic Materials Research and Development-Approaches in Academia and National Laboratory. *Propell. Explos. Pyrot.* **39** (4), 483-485 (2014).
19. Osborne, D.T., Pantoya, M. L. Effect of Al Particle Size on the Thermal Degradation of Al/Teflon Mixtures. *Combust. Sci. Technol.* **179**, 1467-1480 (2007).
20. Pantoya, M. L., Dean, S. W. The influence of alumina passivation on nano-Al/Teflon reactions. *Thermochim. Acta.* **493** (1-2), 109-110 (2009).
21. Mulamba, O., Pantoya, M. Exothermic surface reactions in alumina-aluminum shell-core nanoparticles with iodine oxide decomposition fragments. *J. Nanopart. Res.* **16** (3), 2310 (2014).
22. Nelyubina, Y., Antipin, M. Y., Lyssenko, K. A. Extremely short halogen bond: the nature and energy of iodine-oxygen interactions in crystalline iodic acid. *Mendeleev. Commun.* **21**, 250-252 (2011).
23. Bockmon, B. S., Pantoya, M. L., Son, S. F., Asay, B. W., Mang, J. T. Combustion velocities and propagation mechanisms of meta-stable intermolecular composites. *J. Appl. Phys.* **98** (6), 064903 (2005).
24. Pantoya, M. L., Levitas, V. I., Granier, J. J., Henderson, J. B. Effect of bulk density on reaction propagation in nanothermites and micron thermites. *J. Propul. Power.* **25** (2), 465-470 (2009).